Integrative and Comparative Biology

Integrative and Comparative Biology, volume 61, number 2, pp. 491–505
doi:10.1093/icb/icab096

Society for Integrative and Comparative Biology

SYMPOSIUM

The Stabilizing Function of the Tail During Arboreal Quadrupedalism

Jesse W. Young,[1,*] Brad A. Chadwell,[†] Noah T. Dunham,[‡,§] Allison McNamara,[¶] Taylor Phelps,[*] Tobin Hieronymus[*] and Liza J. Shapiro[¶]

[*]Department of Anatomy and Neurobiology, Northeast Ohio Medical University, Rootstown, OH 44272, USA; [†]Department of Anatomy, Idaho College of Osteopathic Medicine, Meridian, ID 83642, USA; [‡]Department of Conservation and Science, Cleveland Metroparks Zoo, Cleveland, OH 44109, USA; [§]Department of Biology, Case Western Reserve University, Cleveland, OH 44106, USA; [¶]Department of Anthropology, University of Texas at Austin, Austin, TX 78712, USA

From the symposium "An evolutionary tail: Evo-Devo, structure, and function of post-anal appendages" presented at the annual meeting of the Society for Integrative and Comparative Biology, January 3–7, 2021

[1]E-mail: jwyoung@neomed.edu

Synopsis Locomotion on the narrow and compliant supports of the arboreal environment is inherently precarious. Previous studies have identified a host of morphological and behavioral specializations in arboreal animals broadly thought to promote stability when on precarious substrates. Less well-studied is the role of the tail in maintaining balance. However, prior anatomical studies have found that arboreal taxa frequently have longer tails for their body size than their terrestrial counterparts, and prior laboratory studies of tail kinematics and the effects of tail reduction in focal taxa have broadly supported the hypothesis that the tail is functionally important for maintaining balance on narrow and mobile substrates. In this set of studies, we extend this work in two ways. First, we used a laboratory dataset on three-dimensional segmental kinematics and tail inertial properties in squirrel monkeys (*Saimiri boliviensis*) to investigate how tail angular momentum is modulated during steady-state locomotion on narrow supports. In the second study, we used a quantitative dataset on quadrupedal locomotion in wild platyrrhine monkeys to investigate how free-ranging arboreal animals adjust tail movements in response to substrate variation, focusing on kinematic measures validated in prior laboratory studies of tail mechanics (including the laboratory data presented). Our laboratory results show that *S. boliviensis* significantly increase average tail angular momentum magnitudes and amplitudes on narrow supports, and primarily regulate that momentum by adjusting the linear and angular velocity of the tail (rather than via changes in tail posture *per se*). We build on these findings in our second study by showing that wild platyrrhines responded to the precarity of narrow and mobile substrates by extending the tail and exaggerating tail displacements, providing ecological validity to the laboratory studies of tail mechanics presented here and elsewhere. In conclusion, our data support the hypothesis that the long and mobile tails of arboreal animals serve a biological role of enhancing stability when moving quadrupedally over narrow and mobile substrates. Tail angular momentum could be used to cancel out the angular momentum generated by other parts of the body during steady-state locomotion, thereby reducing whole-body angular momentum and promoting stability, and could also be used to mitigate the effects of destabilizing torques about the support should the animals encounter large, unexpected perturbations. Overall, these studies suggest that long and mobile tails should be considered among the fundamental suite of adaptations promoting safe and efficient arboreal locomotion.

Locomotion in an arboreal environment is inherently precarious. The narrow diameter, steep orientation, and increased compliance of arboreal supports present stability challenges that are not typically encountered during movement on the flat ground (although such generalizations are certainly tempered by the interaction between body size and support size in the environment: Jenkins 1974; *Shapiro* et al.

Advance Access publication June 28, 2021

2014). As such, comparative studies have identified a host of morphological and behavioral specializations in arboreal animals broadly thought to promote stability when moving on narrow, steep, and compliant arboreal substrates, including grasping extremities—as well other morphologies to maintain substrate attachment (e.g., the gecko adhesion system: *Russell* et al. 2019), relatively long and mobile limbs, and the use of distinct quadrupedal gait kinematics marked by increased joint compliance and atypical footfall patterns (*Larson* 1998; *Cartmill* et al. 2007; *Lemelin* and Schmitt 2007; *Nyakatura* 2019).

Less well-studied is the role of the tail in maintaining balance during arboreal quadrupedalism. Several anatomical studies have found that arboreal taxa frequently have relatively longer and more massive tails than their terrestrial counterparts (*Horner* 1954; *Martin* 1968; *Wilson* 1972; *Siegel* and van Meter 1973; *Grand* 1977; *Irschick* et al. 1997; *Delciellos* and Vieira 2007; *Hayssen* 2008; *Russo* and Shapiro 2011; *Sheehy et al. 2016*; *Mincer and Russo 2020*), although some phylogenetic comparative research has found this "habitat signal" of tail length to be weak within certain restricted taxonomic groups (*Sehner* et al. 2018; *Weisbecker* et al. 2020). Broadly, two nonmutually exclusive ecomorphological hypotheses have been proposed to explain substrate-driven differences in tail length: (1) arboreal taxa use the tail as a counterweight to help maintain balance when sessile or slowly moving or (2) arboreal taxa use the tail as an inertial appendage to dynamically regulate whole-body angular momentum on precarious supports.

In support of the first hypothesis, field observations have confirmed that arboreal primates tend to sit with their tails extended vertically below the branch, lowering their center of mass and improving balance atop an arboreal support (*Rose* 1974). However, given the likelihood that balance perturbations are greater during locomotion, most biomechanical research of tail function on precarious supports has focused on the possible dynamic benefits. Although such studies are few, most have found that (1) tail movements become more dynamic when balance becomes compromised and, inversely, (2) loss of the tail compromises balance. For example, laboratory studies of cercopithecine monkeys (i.e., *Papio*, *Erythrocebus*, *Chlorocebus*, and *Macaca*) and domestic cats (*Felis catus*) walking over narrow supports use rapid transverse sweeps of the tail muscle activity to control trunk position and maintain mediolateral balance over the support (*Walker* et al. 1998; *Larson* and Stern 2006). In a comparison of tail movements between two similarly sized and closely related platyrrhine species, *Young* et al. (2015) found that tamarins (*Saguinus oedipus*)—a species characterized by claw-like nails, relatively short digits, and a reduced hallux—used much more dynamic tail movements than did squirrel monkeys (*Saimiri boliviensis*), a species with better-developed autopodial grasping morphology, suggesting a functional trade-off between grasping ability and tail use in arboreal quadrupeds. Similarly, data on mouse lemurs (*Microcebus murinus*) moving over a variety of supports show that tail movements become more pronounced on narrower supports (*Shapiro* et al. 2016). Outside of mammals, work by *Jusufi et al.* (2008, 2011) on aerial righting in falling lizards has shown that rapid, dynamic sweeps of tail are critical for reorienting the body for a safe landing.

Experimental studies of the effects of tail loss or immobilization on locomotor stability in animals on precarious supports have generally provided even more dramatic demonstrations of the utility of a long and massive tail in an arboreal environment. For example, *Buck* et al. (1925) and *Igarashi* and Levy (1981) found that mice and monkeys, respectively, had pronounced difficulty maintaining stability on narrow and mobile supports following tail amputation. Similarly, domestic cats whose tails have been paralyzed via sacrocaudal spinal cord transection have significantly greater difficulty recovering from mediolateral perturbations than intact cats (*Walker* et al. 1998). Tail loss impacts arboreal balance even in very small tetrapods (i.e., Anole lizards, *Anolis carolinensis*; *circa* 5 g in body mass). *Hsieh* (2016) found that following tail loss via autotomy, lizards moving on narrow perches exhibited several kinematic adjustments consistent with compensation in decreased locomotor stability. Similarly, in a study of lizards moving around a constructed environment containing a variety of perches, *Ballinger* (1973) found that tailless *A. carolinensis* perched less than intact counterparts and tended to avoid the most precarious substrates when they did perch.

Specifics aims and hypotheses

As reviewed above, anatomical comparative studies have demonstrated that arboreal taxa frequently have longer and more massive tails than their closely related terrestrial counterparts. Laboratory studies of tail kinematics and the effects of tail reduction have presented data commensurate with the hypothesis that the tail is functionally important for maintaining balance on precarious substrates. In this set of studies, we extend this work in two ways. First, we use a laboratory dataset on three-dimensional (3D) segmental kinematics and inertial properties in

squirrel monkeys (*S. boliviensis*) as a model system to investigate how arboreal animals modulate tail angular momentum during steady-state locomotion, predicting that tail angular momentum should be greater on narrow supports and should be directly proportional to the overall distance between the tail center of mass and the whole-body center of mass (i.e., proportional to the degree of tail extension), tail linear velocity, and tail angular velocity.

In the second study, we use a quantitative dataset on quadrupedal locomotion in wild platyrrhine monkeys to investigate how free-ranging arboreal animals modulate tail movements in response to substrate variation, with a focus on kinematic measures functionally validated in laboratory studies of tail dynamics (including the data presented here). We predicted that wild monkeys would exhibit greater amplitudes of tail movement and more extended tail postures on narrower and more compliant substrates.

Methods

Methods for both studies are summarized below. More detailed descriptions are provided in the Supplementary Online Methods file.

Study 1: Tail angular momentum in squirrel monkeys (*S. boliviensis*)

Animals

Data were collected from two juvenile female *S. boliviensis* (body mass range: 474–530 g; age: 1.9–2.2 years). Given an average female adult body mass of 711 g (*Smith* and Jungers 1997), the animals in our sample had reached approximately 67–75% of their terminal size. Relative to wild populations of *S. boliviensis*, this would approximate an age past the average weaning age of 12–18 months, but before the average age at first reproduction at 3.5 years Zimbler-Delorenzo and Stone 2011). The Northeast Ohio Medical University (NEOMED) Institutional Animal Care and Use Committee (IACUC) approved all procedures before the beginning of this research.

Morphometric data collection

We estimated segmental inertial properties using a combination of cadaveric dissection and geometric modeling (*Raichlen* 2004). Although our hypothesis testing only required data on tail inertial properties, we measured all body segments to facilitate comparisons. Segmental mass distributions were quantified by disarticulating an adult male *S. boliviensis* cadaver (body mass: 943.4 g). This animal was not part of the sample studied in locomotor experiments. Anatomical landmarks used to identify each segment are listed in Supplementary Table S1. We measured each segment mass to the nearest tenth of a gram using an electronic balance. Segmental mass moments of inertia were quantified from measurements of segment lengths and diameters in the two monkeys included in our locomotor sample, following the equations in *Raichlen* (2004). We subsequently adjusted initial estimates of segmental mass moments of inertia to parallel the segment mass distributions measured from the cadaveric dissections, assuming isometry. The final dataset of *S. boliviensis* inertial properties is detailed in Table 1. We also quantified static whole-bodycenter of mass (CoM) position using the reaction board method (for details, see *Young* 2012). Static CoM position in the two monkeys, across a range of limb, trunk and tail postures (i.e., flexed, extended, or neutral), averaged 57.1% (range: 50.0–59.7%) and 62.3% (range: 57.0–62.7%) of trunk length from the shoulders to the hips for the two individuals.

Locomotor data collection

To aid in later video tracking and kinematic analysis, monkeys were anesthetized with isoflurane before each experiment to apply circular reflective markers to the lateral surfaces of the limb joints and at three points along the length of the tail (*Fig. 1a*; Supplementary Video S1). Following marker placement, we recorded body mass to the nearest gram using an electronic balance. Animals were encouraged to cross 4 m long sets of 5 cm, 2.5 cm, or 1.25 cm diameter horizontal poles at self-selected speeds. These diameters are representative of substrates utilized in the squirrel monkey's natural habitat (*Boinski* 1989; *Dunham* et al. 2018, 2019a; *McNamara* et al. 2019). Four high-speed digital cameras (Xcitex XC-2; Xcitex Inc., Woburn), two on each side of the runway, recorded video at 200 Hz as the animal crossed over the force-sensitive region. See *Chadwell* and Young (2015) for a more detailed description of the locomotor data collection protocol. In total, we collected data on 87 locomotor strides, including 29 on the 5-cm pole, 28 on the 2.5-cm pole, and 30 on the 1.25-cm pole.

Quantification of segmental kinematics and angular momenta

All locomotor analyses were performed using MATLAB (Mathworks, Natick, MA) routines, custom-written by BAC. To track and quantify the 3D locomotor kinematics from both the left and right sides of the animals, we calibrated the temporally synchronized images from the four cameras to

Table 1 Size-adjusted segmental inertial properties in *S. boliviensis*

Segment	Relative mass[a] (%)	Relative I_{CoM}[b] (%)
Head	8.0	1.8
Trunk	43.4	100.0
Arm	2.7	1.1
Forearm	1.7	0.7
Hand	0.7	0.03
Thigh	10.3	5.3
Leg	4.4	2.8
Foot	1.9	0.6
Proximal tail	4.1	12.2
distal tail	1.1	3.2

aSegment mass as a percentage of whole-body mass. Limb segment masses only represent one side of the body.
bSegment mass moment of inertia about its center of mass along the proximodistal axis, expressed as a percentage of the largest segmental I_{CoM} (i.e., that of the trunk). Mass moments of inertia were estimated from measurements of the two individuals in our locomotor sample using a geometric model (Raichlen 2004) and then isometrically scaled to mirror the segmental mass distribution measured from the cadaveric dissection.

the same coordinate space using previously published calibration protocols (*Standen* and Lauder 2005; *Chadwell* and Young 2015; *Young* et al. 2016; *Dunham* et al. 2019b). We then digitized 3D position of the hips, shoulders, and three tail markers on both sides of the body using ProAnalyst v. 1.6 motion analysis software (Xcitex Inc., Woburn, MA) (Fig. 1b). Shoulder and hip marker trajectories were used to estimate instantaneous whole-body CoM position throughout each frame of the stride, as:

$$\vec{m}_{sh} + (\vec{m}_{hp} - \vec{m}_{sh}) \cdot p_{CoM}, \quad (1)$$

where $\vec{m}_{sh}$ and $\vec{m}_{hp}$ equal the midpoint of the between the left and right shoulder and hip vectors, respectively, and p_{CoM} is the static position of the CoM, expressed as a percentage of trunk length from the shoulders to the hips (calculated as described above).

We estimated the segmental angular momentum of the tail segments in the pitch plane (i.e., L_{pitch}, arising from tail movement in the *xz*-/sagittal plane; Fig. 1b) and the yaw plane (i.e., L_{yaw}, arising from tail movement in the *xy*-/coronal plane) on a frame-by-frame basis using the equation:

$$\vec{L}_i\left(\vec{r}_p\right) = \left(\vec{r}_{CoM,i} - \vec{r}_p\right) \times m_i\vec{v}_{CoM,i} + I_i\vec{\omega}_i. \quad (2)$$

On the left-hand side of this equation, $\vec{L}_i$ represents the angular momentum of the *i*-th segment relative to a reference point position vector ($\vec{r}_p$). We used the instantaneous whole-body CoM position as the reference point for all frame-by-frame calculations. On the right-hand side of this equation, $\vec{r}_{CoM,i}$ is the position vector of the tail segment's CoM relative to the whole-body CoM, m_i is the segment mass, $\vec{v}_{CoM,i}$ is the velocity vector of the segment's CoM, I_i is the segment's mass momentum of inertia, and $\vec{\omega}_i$ is the segment's angular velocity

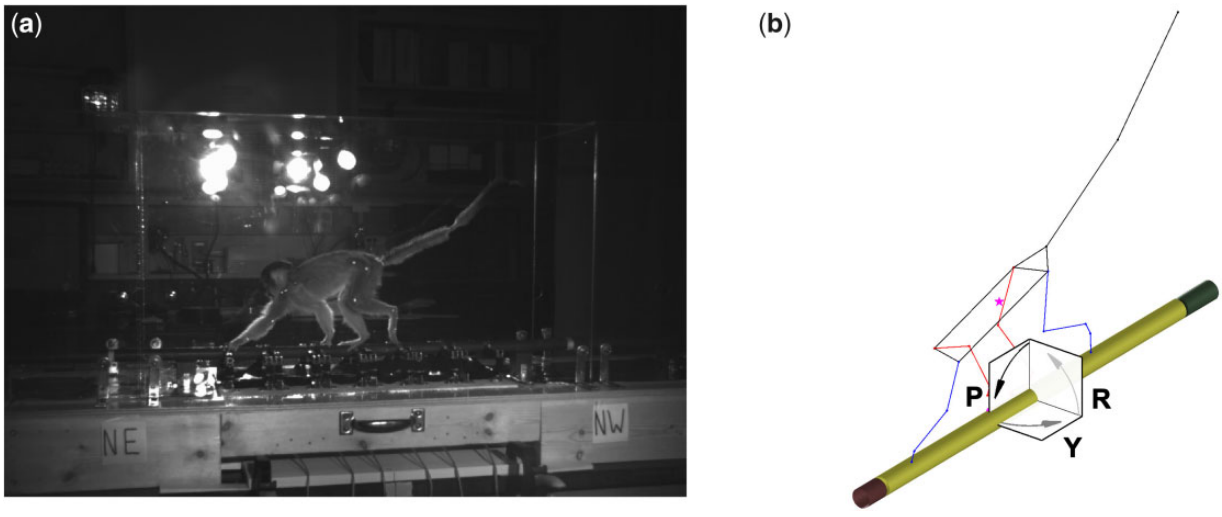

Fig. 1 Video-based analysis of 3D tail kinematics in *S. boliviensis*. (**a**) Exemplar video frame of juvenile squirrel monkeys (*S. boliviensis*, body mass = 492 g) crossing the 2.5 cm diameter experimental support. Note the reflective markers on all limb joints and three locations along the tail used to calculate segment position. (**b**) A wireframe animation showing the reconstructed position of the squirrel monkey's limbs, trunk, and tail segments. The large star within the trunk shows the computed position of the whole-body center of mass. Rectangles representing the pitch (P), yaw (Y), and roll (R) planes are drawn at the origin of the pole-centered coordinate system. Arrows indicate the direction of the positive rotation in each plane.

about its own CoM (*Elftmann* 1939; *Herr* and Popovic 2008; *Chiovetto* et al. 2018). Because we lacked data on tail I_{CoM} about the long axis of the segment, we estimate L_{roll} from the first summand of Equation (2) (i.e., without $I_i\vec{\omega}_i$). However, given the unlikelihood that the tail can freely rotate about its long axis, our estimate of L_{roll} should be accurate nonetheless. For all planes, we calculated the angular momentum of the proximal and distal tail segments independently and then summed these values within each video frame to calculate the angular momentum of the tail as a unified segment.

Statistical analyses

Variation in tail angular momentum associated with support diameter or movement plane was assessed using mixed-effects analyses of covariance (ANCOVA). The individual animal was included as a random factor in all regression models. All continuous variables were log-transformed before analysis to improve normality. We first fit the full model, including support diameter and movement plane (i.e., pitch, yaw, and roll) as main effects, average stride speed (quantified based on the displacement of the calculated whole-body CoM) as a covariate, and all possible factor interactions. We then simplified each ANCOVA model by removing nonsignificant interactions (*Crawley* 2007). In cases of significant factor-by-covariate interactions, we *post hoc* tested for significant differences between factor levels at the minimum, mean, and maximum values of the speed range common across all experimental conditions.

We evaluated how *S. boliviensis* modulated mean (unsigned) tail angular momentum and tail angular momentum amplitudes using mixed-effects multiple regressions. The random factor for these mixed-effects models was individual trial number nested within the animal. We scaled and centered all variables (i.e., converted them to z-scores) before analysis, facilitating comparisons of standardized partial regression coefficients (i.e., $_{\beta}$-weights) among predictors. Coefficients of determination (i.e., R^2) were determined following *Nakagawa* et al. (2017).

The sample size for this study was necessarily limited by the logistical difficulties of obtaining and housing non-human primates. As such, we also provide estimates of intraclass correlations (ICCs) for all mixed-effects ANCOVAs and regression models to gauge the degree to which observed patterns of association differed between the two individuals. Intraclass correlations are essentially scaled variance components and quantify the proportion of overall dependent variable variance due to differences between individuals.

We discuss the broad outcomes of each statistical test in Results section. Detailed information on each test is presented in Supplementary Tables S3 and S4.

Study 2: Tail kinematics in wild platyrrhine monkeys

Field sites and study subjects

Data were collected on free-ranging primate species at two field sites: Tiputini Biodiversity Station in Ecuador from August–October 2017 (corresponding to the end of the dry season) (*Marsh* 2004) and La Suerte Biological Field Station in Costa Rica from June to July 2018 (corresponding to the beginning of the wet season) (*Garber* et al. 2010). In total, we recorded individuals from habituated and semi-habituated groups of 4–40+ individuals belonging to 12 species, including members of Atelidae (*Ateles belzebuth*, *Ateles geoffroyi*, *Lagothrix lagotricha*, *Alouatta palliata*, and *Alouatta seniculus*), Cebinae (*Cebus capucinus*, *Cebus albifrons*, and *Saimiri sciureus*), Callitrichinae (*Saguinus tripartitus* and *Cebuella pygmaea*), and Pitheciidae (*Pithecia aequatorialis* and *Callicebus discolor*) (see Supplementary Table S2 for details about group sizes for each species). *Ateles geoffroyi*, *Alouatta palliata*, and *Cebus capucinus* were filmed at La Suerte; the remaining nine species were filmed at Tiputini. Previously published studies of this dataset have considered aspects of habitat usage and gait kinematics (*Dunham* et al. 2018, 2019a; *McNamara* et al. 2019; *Dunham* et al. 2020), but not tail behavior *per se*. In total, we coded 660 locomotor strides. A chronogram of the species included in our sample, along with the mean body mass and the total number of strides for each species, is shown in *Fig. 2*. All procedures for this study were approved by NEOMED IACUC and Ecuador Ministerio del Ambiente (permit no. 014-2017-IC-DPAO/AVS) before beginning this research.

Field data collection

We have described our field data collection protocol in detail elsewhere (*Dunham* et al. 2018; see also Supplementary Online Methods). We opportunistically filmed monkeys moving quadrupedally in different forest strata and on substrates of varying diameter and type (i.e., branch, palm frond, liana, or bamboo). We quantified the average diameter of each locomotor substrate using remote sensing techniques (see *Dunham* et al. 2018 and Supplementary Online Methods for more details). Substrate diameters were subsequently scaled to the cube root of average species body mass (taken from *Smith* and Jungers 1997) to adjust for size variation among our focal taxa.

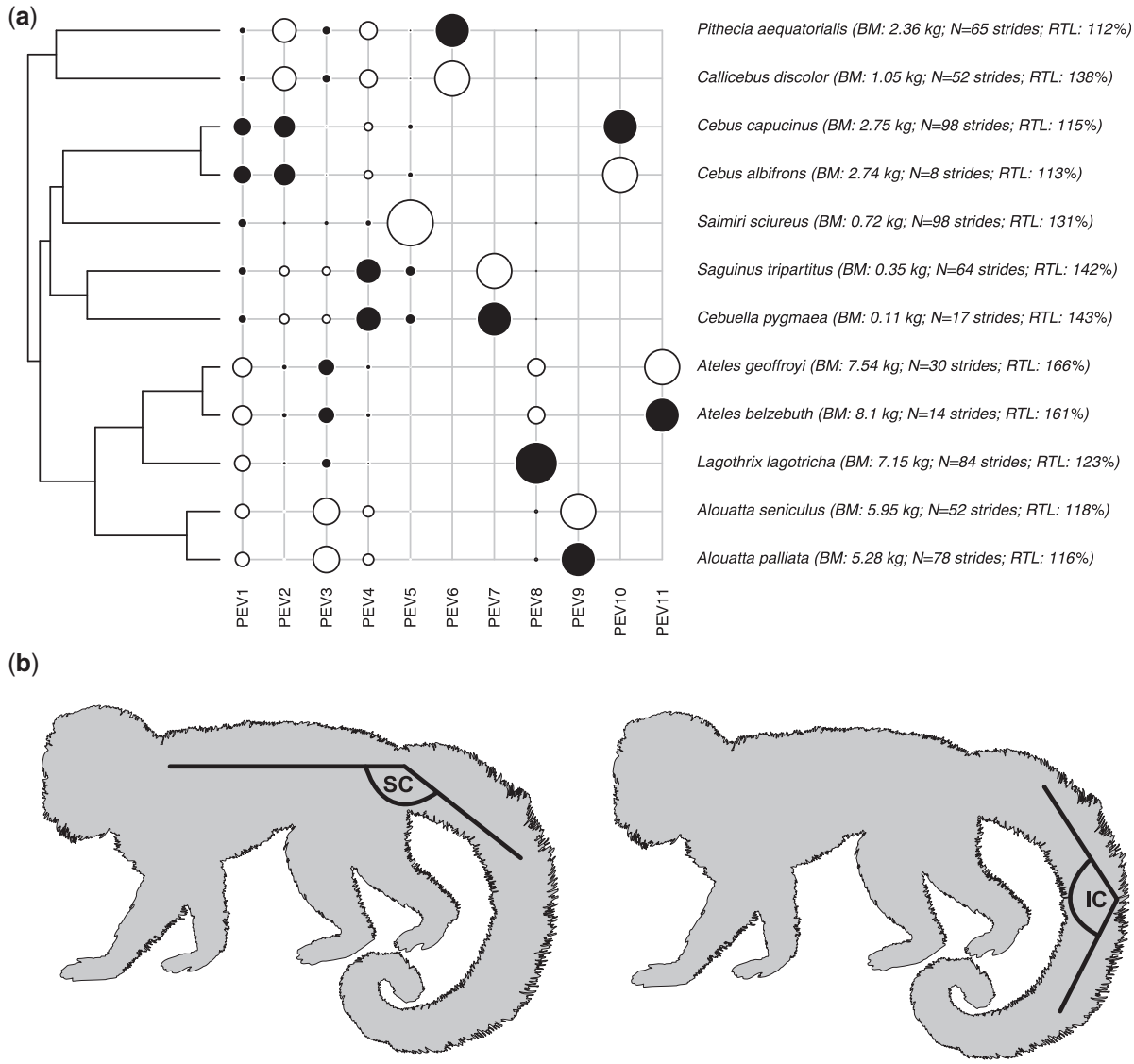

Fig. 2 (**a**) Phylogram and the 11 PEV contrasts for the 12 platyrrhine taxa included in our dataset. White circles indicate negative values and black circles positive values along the respective PEV axes, such that PEV1 primarily differentiates atelids from the other clades, PEV2 primarily differentiates Pithecids from Cebines, and so on. The diameter of the circle is representative of the amplitude of the PEV (i.e., indicative of the loading of the indicated phylogenetic contrast along the axis). Eigenvector amplitudes were scaled to the square root of their respective eigenvalues to facilitate proportional comparisons among PEVs. Body masses are taken from Smith and Jungers (1997). (**b**) Schematic descriptions of sacrocaudal posture ("SC") and intracaudal posture ("IC"). See text for further description. Public domain monkey silhouette used with permission from PhyloPic.org.

Data analysis

We used three complementary measures to describe tail posture and tail displacement throughout each stride in our database. First, for each frame of the stride, we qualitatively coded tail posture as either flexed or extended both relative to the trunk (i.e., sacrocaudal joint posture) and within the tail itself (i.e., net intracaudal joint posture) (see Fig. 2(b) for schematic descriptions of each measure). We subsequently used these qualitative frame-by-frame ratings of tail posture to calculate the percent of stride duration in which the tail was held in an extended sacrocaudal posture (i.e., in line with or dorsal to the trunk) as well as the percent of stride duration in which the intracaudal joints were predominantly extended. We refer to these measures as "%sacrocaudal extension" and "%intracaudal extension." Finally, we quantified the magnitude of tail displacement during the stride by first measuring the Euclidean distance between the tail base and the tail tip and scaling this distance to body length (i.e., nose tip to the base of tail; both values in pixels) on a frame-by-frame basis, thus calculating a size-adjusted measure of effective tail length for

each frame in the stride. The amplitude of this metric, referred to here as "relative tail displacement," is our measure of overall tail movement. We excluded any trials from the dataset in which the tail was actively grasping the support.

In addition to the tail metrics, we also quantified relative speed across the stride by measuring the displacement of the animal's nose during stride as a percentage of body length and dividing this value by stride duration (*Dunham* et al. 2019a). Finally, we measured the amplitude of support displacement during the stride as a means of empirically quantifying substrate compliance. We digitized two points within each frame of the stride: one easily identifiable point roughly centered on the locomotor substrate (e.g., a fork in the branch or a distinct change in coloration) and a stationary point independent of the locomotor substrate (e.g., trunk or branch of an adjacent tree). The maximum amplitude of locomotor substrate displacement was quantified relative to the stationary point and scaled to the animal's body length (both values measured in pixels).

Statistical analyses

We used phylogenetic eigenvector (PEV) analysis to investigate the possible influence of phylogenetic relatedness on patterns of tail usage in our focal species (Diniz et al. 2015). The chronogram used to construct PEVs was sampled from the consensus phylogeny of the 10k trees project (Arnold et al. 2010). More information about using this method in the context of our wild primate dataset is provided in Dunham et al. (2019a).

We used multiple regressions to empirically assess the determinants of variation in %sacrocaudal extension, %intracaudal extension, and relative tail displacement, entering relative speed, relative substrate diameter, relative substrate displacement, and all PEVs as predictor variables in the regression models. To investigate how morphological variability among the wild monkeys might influence tail kinematics, we also included relative tail length (RTL) as a predictor variable in all multiple regression models. RTL was calculated by expressing tail length as a percentage of head + trunk (i.e., body) length, using species mean data collected from *Mittermeier* et al. (2013). All predictor variables except for the PEVs were Box–Cox transformed to improve normality, and all predictor variables were converted to *z*-scores before analysis. Full multiple regression models including all predictor models were reduced using an iterative stepwise procedure seeking to maximize the model's Akaike Information Criterion (i.e., the "stepAIC" procedure from the MASS package in R) to arrive at a simplified model for each dependent variable. Finally, simplified models were refit as mixed-effects models, specifying individual movie clip as a random variable, thus controlling for possible psuedoreplication arising from the inclusion of multiple strides from the same bout of locomotion.

Results

Study 1: Tail angular momentum in squirrel monkeys (*S. boliviensis*)

The monkeys in our locomotor sample had an average head length + trunk length of 249 mm and an average tail length of 417 mm, such that the tail was 167% of overall body length. Data on segmental inertial properties are listed in Table 1. Although we focus only on tail angular momentum in this study, we include inertial property data for all other segments to facilitate comparison. The trunk is the largest segment, constituting 43.4% of body mass, and has the greatest estimated I_{CoM} (all other I_{CoM} are scaled to the trunk value). Although the tail accounts for only 5.3% of body mass, the elongate shape of the segment gives it the second greatest I_{CoM} of all segments (i.e., >15% of trunk mass moment of inertia).

Time series of tail angular momenta in the pitch, yaw, and roll planes are illustrated in *Fig. 3*. Generally, L_{pitch} followed a double sine wave profile with four extrema (i.e., two maxima and two minima; range: 2–10 extrema, mean: 4.4), likely associated with the rise and fall of the whole-body CoM during the two forelimb/hindlimb support periods that characterize symmetrical quadrupedal gaits (*Schmitt* et al. 2006). In contrast, L_{yaw} and L_{roll} were more variable (L_{yaw}: 1–25 extrema, mean: 4.9; L_{roll}: 2–27 extrema, mean: 5.7), although their time-series broadly followed a sinusoidal profile during each stride, transitioning from positive to negative, or positive to negative, as the tail swept from side to side. Given the variability in the predominant direction of L_{yaw} and L_{roll} across strides, mean time series curves for these variables do not show a consistent pattern.

Results of our ANCOVA models of mean tail angular momentum and tail angular momentum amplitude across strides are plotted in *Fig. 4* and summarized in Supplementary Table S3 and S4. Mean tail angular momentum and tail angular momentum amplitude significantly increased with speed ($P \leq 0.011$). On average, tail angular momentum magnitudes were greatest for L_{pitch} and lowest for L_{roll}, with L_{yaw} intermediate to the other two ($P \leq 0.003$). Tail angular momentum amplitudes

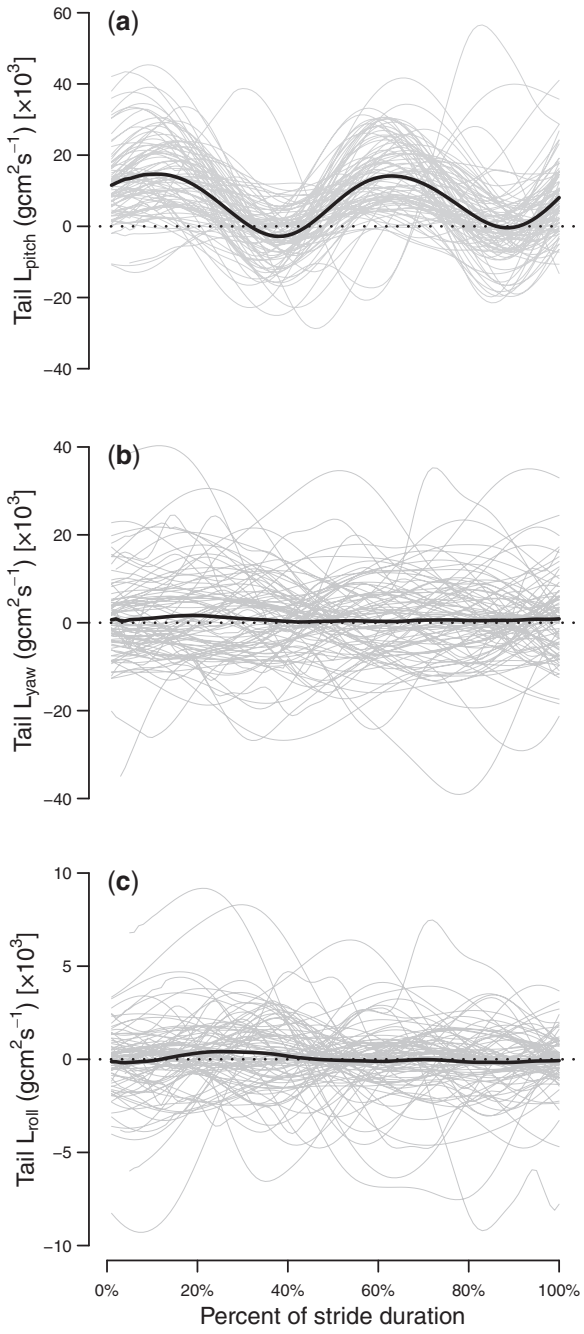

Fig. 3 Tail angular momentum profiles in the pitch (**a**), yaw (**b**), and roll (**c**) planes for *S. boliviensis*. Solid black lines indicate the mean profile across all strides, whereas narrow gray lines represent momentum profiles for individual strides. See Fig. 1(b) for a schematic illustration of how pitch, yaw, and roll measurement planes were defined.

followed this same pattern ($P \leq 0.003$), although the extent of the difference varied among substrate diameters, as demonstrated by a significant diameter-by-movement plane interaction ($P = 0.03$). Regardless of movement plane, mean tail angular momentum magnitudes were lowest on the broad 5 cm support ($P \leq 0.044$) and did not differ between the two smaller supports. Similarly, tail angular momentum amplitudes were greatest on the smallest 1.25 cm support and least on the broad 5 cm support, with values on the 2.5 cm support generally intermediate between the other two ($P \leq 0.039$), although L_{pitch} amplitudes did not differ between 5 cm and 2.5 cm poles.

Results of our multiple regression analyses of the determinants of variation in the mean and amplitude of L_{pitch}, L_{yaw}, and L_{roll} are summarized in Table 2. Across all movement planes, the average magnitude and total amplitude of tail angular momentum significantly increased with increasing linear velocity ($P \leq 0.004$), and generally increased with increasing tail angular velocity for all variables except mean L_{pitch} ($P \leq 0.011$ for all significant relationships). The influence of tail CoM distance on tail angular momentum was more nuanced. Mean tail CoM distance was only related to mean tail angular momentum in the rolling plane ($P = 0.014$). The amplitude of tail CoM distance was significantly positively correlated with L_{pitch} amplitudes and significantly negatively correlated to L_{roll} amplitudes (both $P < 0.001$), although uncorrelated with L_{yaw} amplitudes.

In summary, the results of Study 1 demonstrate that *S. boliviensis* significantly increases average tail angular momentum magnitudes and amplitudes on narrow supports and primarily regulates tail angular momentum by adjusting the linear and angular velocity of the tail. We build on these findings in Study 2 by examining how wild platyrrhine monkeys modulate tail position and tail displacement in response to variation in substrate precarity.

Study 2: Tail kinematics in wild platyrrhine monkeys

Results of our final multiple regression analyses of variation in wild platyrrhine tail posture and displacement, following stepwise model selection, are plotted in *Fig. 5* and summarized in Table 3. The modal extension of the tail relative to the trunk (i.e., %sacrocaudal extension) significantly increased with relative speed ($P < 0.001$; Fig. 5a). The net posture of the intracaudal joints (i.e., %intracaudal extension) became significantly more flexed with increasing relative substrate diameter ($P = 0.013$; Fig. 5c), indicating that the monkeys tended to have more extended tails on narrower supports. Finally, relative tail displacement significantly decreased with increasing relative substrate diameter ($P = 0.004$; Fig. 5e) and significantly increased with increasing substrate displacement ($P < 0.001$; Fig. 5f), such that the tail movements became more exaggerated on narrower and more mobile supports. Finally, all three

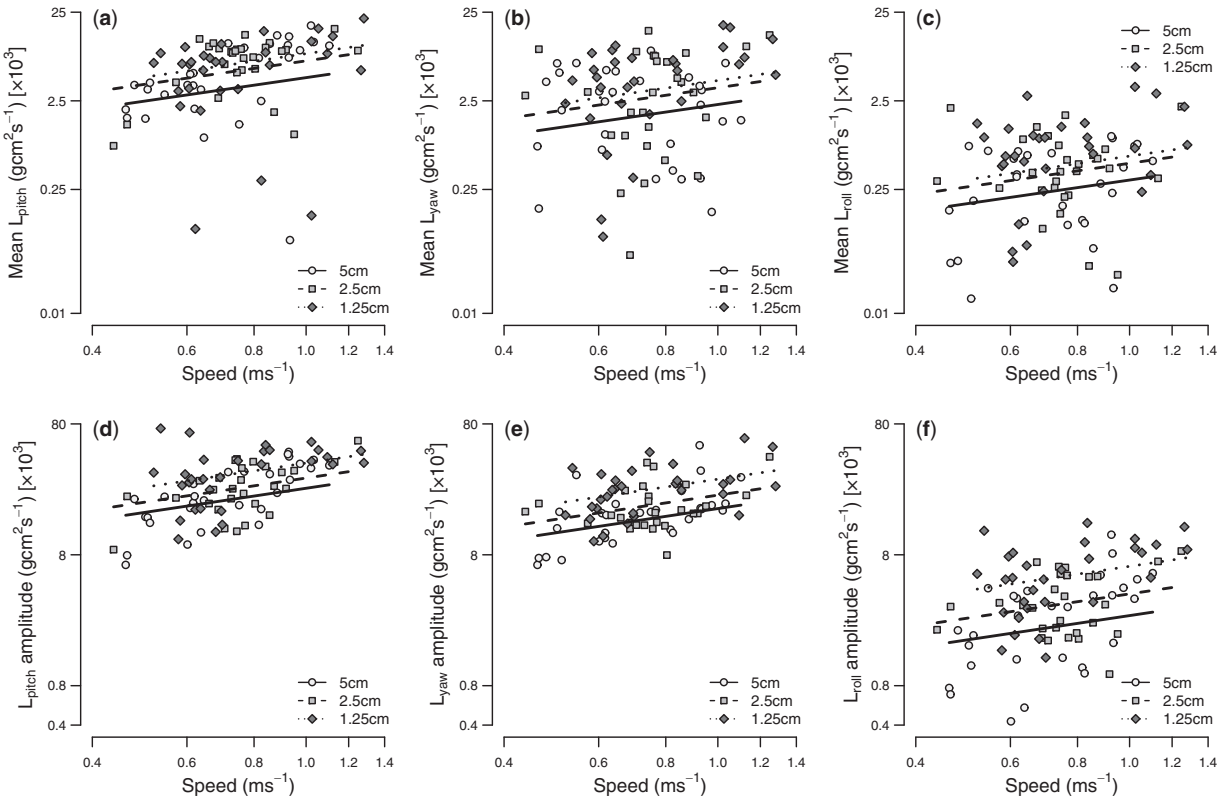

Fig. 4 Variation in *S. boliviensis* tail angular momentum among support diameters and movement planes, plotted against average speed. Mean values (unsigned; panels **a–c**) and total amplitudes (panels **d–f**) of tail angular momentum across individual strides are shown for the pitch (panels **a** and **d**), yaw (panels **b** and **e**), and roll (panels **c** and **f**). Trend lines indicate mixed-effects model fits within diameters. Variates are plotted on log–log axes.

measures were significantly related to RTL (Fig. 5b, d, and f; all $P < 0.001$), indicating that relatively long-tailed species tended to move with more extended tails and exhibit greater amplitudes of tail movement. We also note that various phylogenetic eigenvectors significantly explained variation in all tail kinematic variables, indicating a strong phylogenetic component to the tail kinematics of wild platyrrhines.

Discussion

A tail length equal to 167% of body length places *S. boliviensis* among the longest-tailed animals (for their body size) in the broad comparative studies of *Sehner* et al. (2018) and *Mincer* and Russo (2020), suggesting that the tail is functionally important to this species. The pronounced tail length undoubtedly contributed to its relatively large mass moment of inertia—the largest I_{CoM} of all body segments except the trunk. Overall, we found that the tail had a tapered proximo-distal profile, such that the mass of the distal segment was roughly a quarter that of the proximal. The larger bulk of the proximal segment may be due to the more proximal location of the caudal musculature in nonprehensile tailed monkeys (*Lemelin* 1995).

Regardless of substrate diameter, we found that in *S. boliviensis* average tail angular momentum and tail angular momentum amplitude was highest in the pitch plane and least in the roll plane, with yaw plane values occupying an intermediate position. Kinetic data from the same *S. boliviensis* dataset show that this angular momentum hierarchy across tail movement planes roughly corresponds to the magnitude of substrate reaction forces—and thus external moments—acting on the whole-body CoM in the vertical, fore-aft, and mediolateral directions (i.e., vertical forces > fore-aft forces > mediolateral forces). Specifically, average peak forces as a percent of body weight were 121% on the vertical axis [95% confidence limits (CL) 119–123%], 16.6% on the fore-aft axis (95% CL 15.5–17.7), and only 5.65% on the mediolateral axis (95% CL 5.24–6.06%) (see also *Young* and Chadwell 2020). The overall pattern of association between the magnitudes of tail angular momenta and corresponding substrate reaction forces suggests that the tail may be acting as a passive mass damper. Under this hypothesis, tail movements would be passively driven by the acceleration

Table 2 Mixed-effects multiple regression models of variation in the mean and amplitude of tail angular momentum[a]

Term	β-weight	P value**	R^2	ICC[b]
Mean L_{pitch}				
Mean tail CoM distance	−0.125	NS	0.310	
Mean tail linear velocity	0.561	**<0.001**		0.110
Mean tail angular velocity	−0.009	NS		
Mean L_{yaw}				
Mean tail CoM distance	−0.068	NS	0.218	
Mean tail linear velocity	0.375	**0.002**		0.117
Mean tail angular velocity	0.268	**0.011**		
Mean L_{roll}				
Mean tail CoM distance	0.267	**0.014**	0.355	0.031
Mean tail linear velocity	0.443	**<0.001**		
L_{pitch} amplitude				
Tail CoM distance amplitude	0.265	**<0.001**	0.432	
Tail linear velocity amplitude	0.309	**<0.001**		0.792
Tail angular velocity amplitude	0.602	**<0.001**		
L_{yaw} amplitude				
Tail CoM distance amplitude	0.110	NS	0.516	
Tail linear velocity amplitude	0.262	**0.004**		0.000
Tail angular velocity amplitude	0.555	**<0.001**		
L_{roll} amplitude				
Tail CoM distance amplitude	−0.237	**<0.001**	0.746	0.023
Tail linear velocity amplitude	0.900	**<0.001**		

[a]All mean values were unsigned (i.e., the absolute value of original measure).
[b]Intraclass correlation coefficients, defined as the proportion of total variance accounted for by interindividual difference.
*Bold values indicate significance at the $P < 0.05$ level; NS = not significant.

of the more cranial portions of the body acting on the tail via the damped spring-like articulation of the sacrocaudal joint. In this manner, the tail would function similarly to the upper limb of walking and running humans (*Collins* et al. 2009; *Pontzer* et al. 2009) or the neck of walking giraffes (*Basu* et al. 2019)—a large inertial mass that can be used to dampen the oscillation of the rest of the body. Further modeling studies, ideally supplemented by electromyographic studies of tail muscle firing patterns (e.g., *Wada* et al. 1993), would be required to test this hypothesis. It could also be true that we would have documented more pronounced, and perhaps actively driven, tail movements if we had challenged whole-body stability via perturbation, rather than focused on steady-state locomotion, or if we had chosen a focal species with less well-development grasping extremities. Previous studies have highlighted the possibility of a functional trade-off between tail usage and grasping ability in arboreal primates, such that an animal with more poorly developed grasping extremities may have been more dependent on actively driven tail movements to maintain stability (*Begun* et al. 1994; *Cartmill* and Milton 1977; *Kelley* 1997; Almécija et al. 2007; *Young* et al. 2015). Indeed, we found that across all movement planes *S. boliviensis* significantly increased the magnitude and amplitude of tail angular momentum on the narrowest supports, consistent with the hypothesis that tail movements may be particularly critical when the balance is challenged.

An animal fundamentally has five strategies through which to increase segmental angular momentum: increase the vector distance between the segment's CoM and the whole-body CoM, increase the linear velocity of the segment, increase the angular velocity of the segment, increase segment mass, or increase the segment's moment of inertia about its CoM (Equation (2); *Elftmann* 1939; *Herr* and Popovic 2008; *Chiovetto* et al. 2018). Since an animal cannot alter segmental inertial properties on an immediate time scale, we focused on the three kinematic strategies. We found that across all

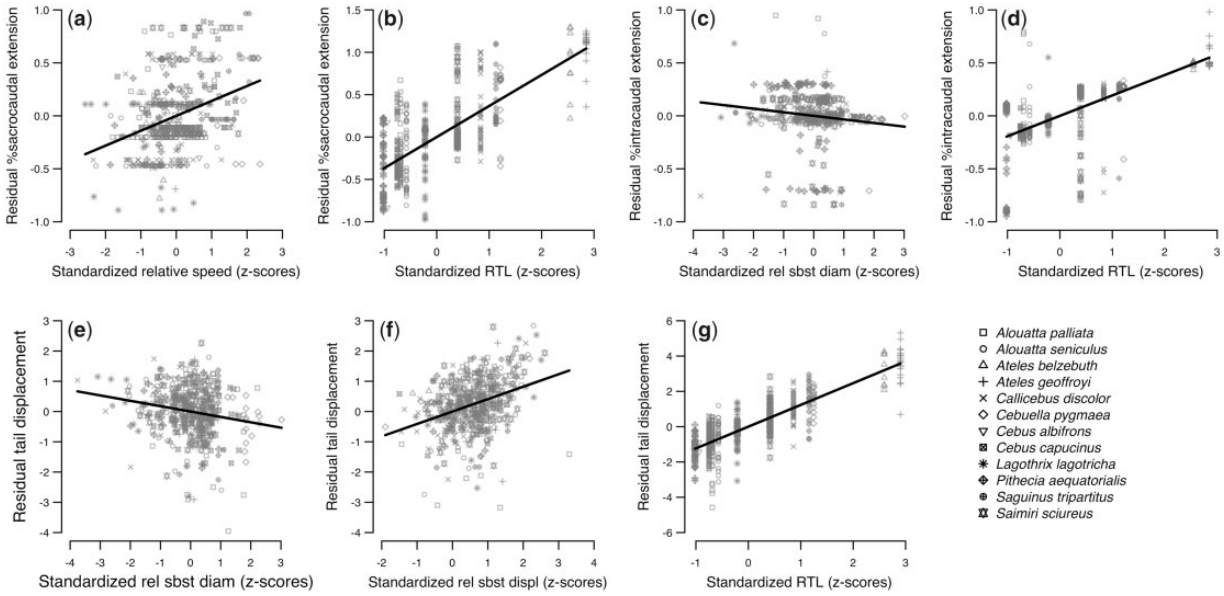

Fig. 5 Substrate- and morphology-related variation in tail kinematics in wild platyrrhine primates. Panels illustrate partial residual plots of significant predictors of sacrocaudal posture (panels **a** and **b**), intracaudal posture (panels **c** and **d**), and relative tail displacement (panels **e–g**), following stepwise model selection (see text and Table 3 for details on the underlying linear regression models). Trend lines indicate the independent relationship between each predictor variable and the dependent variable, conditioned on all of the other predictors in the model. All variables were converted to *z*-scores before analysis.

movement planes, *S. boliviensis* primarily modulated angular momentum by altering segmental linear and angular velocities, rather than tail CoM distance from whole-body CoM *per se*. The lack of association between angular momentum magnitudes/amplitudes and tail CoM position is likely due to *S. boliviensis* consistently maintaining a fairly extended tail (Fig. 1; Supplementary Movie S1). Effective tail length (i.e., Euclidean distance between the base and tip of the tail, divided by total tail length) averaged 78% across the dataset (95% CI 78.6–79.3%), meaning that *S. boliviensis* consistently held the tail at nearly 80% of its fully extended length. Modulating angular momentum via changes in tail CoM position would require frequent flexion and extension of the tail in multiple planes, and may thus be an energetically more costly—or just more convoluted—control strategy than simply adjusting the tail velocity via contraction of extrinsic caudal musculature. Maintaining an extended posture would proportionally increase the effectiveness of any tail movements in the pitch and yaw planes by increasing the distance between the tail and whole-body CoMs—analogous to a tightrope walker using slight movements of a long balancing pole to maintain rolling plane stability atop their narrow perch. Mathematical and physical models (i.e., robotic simulations) of leaping lizards and running cheetahs have also shown the tail's effectiveness in reorienting maneuvers is directly proportional to the distance of the tail CoM from that of the rest of the body (i.e., thus proportional tail length and tail extension) (*Briggs et al. 2012*; *Libby* et al. 2012; *Patel and Braae 2013*).

Our second study showed that wild platyrrhines responded to the precarity of narrow and mobile substrates by extending the intracaudal joints and exaggerating tail displacements (Fig. 5), providing ecological validity to laboratory studies of tail mechanics. The kinematic strategies documented in the wild monkeys would have the effect of increasing the distance between the tail CoM and the whole-body CoM as well as increasing tail linear/angular velocity, facilitating the tail's ability to exert stabilizing angular momentum to the rest of the body. Our inability to detect a substrate-related signal in sacrocaudal joint posture could be associated with the variable angular orientations of the locomotor substrates. The effectiveness of a dorsally canted tail posture would likely vary depending on the orientation of gravity relative to the support. For example, for an animal ascending or descending a steeply angled support, a dorsally extended tail may actually compromise stability by moving the whole-body CoM further from the support, causing the animal to pitch from the support.

We also found that sacrocaudal and intracaudal joint extension, as well as overall tail displacement, were all positively associated with increases in RTL,

Table 3. Final multiple regression models of variation in wild platyrrhine tail posture and displacement, following AIC-based stepwise simplification of full models and refitting as mixed-effects models with individual movie clip included as a random factor.

Model	*β*-weights	*P*-value*	R^2
%Sacrocaudal extension			
Relative speed	0.141	**<0.001**	0.412
Relative tail length	0.367	**<0.001**	
PEV 2	0.070	**0.019**	
PEV 3	-0.057	0.143	
PEV 4	0.233	**0.001**	
PEV 5	0.050	**0.012**	
PEV 6	0.162	**<0.001**	
PEV 7	0.055	**<0.001**	
PEV 8	0.276	**<0.001**	
PEV 9	-0.053	**<0.001**	
PEV 10	-0.067	0.115	
%Intracaudal extension			
Relative substrate diameter	-0.033	**0.013**	0.800
Relative tail length	0.223	**<0.001**	
PEV 1	0.306	**<0.001**	
PEV 2	-0.306	**<0.001**	
PEV 3	-0.152	**<0.001**	
PEV 5	-0.077	**<0.001**	
PEV 6	0.044	**0.001**	
PEV 8	0.116	**<0.001**	
Relative tail displacement			
Relative substrate diameter	-0.163	**0.002**	0.202
Relative substrate displacement	0.408	**<0.001**	
Relative tail length	0.380	**<0.001**	
PEV 3	-0.119	**0.038**	
PEV 4	-0.182	**0.010**	
PEV 5	-0.105	**0.014**	
PEV 6	0.157	**0.004**	
PEV 8	0.176	**0.003**	
PEV 9	-0.073	0.088	

NS = not significant

*Bold values indicate significance at the $p < 0.05$ level.

even after controlling for variation due to locomotor speed, substrate properties, or phylogenetic relatedness. The species with the longest tails for their body size were the ones that most consistently used the tail in a manner that would effectuate the robust production of tail angular momentum.

Finally, as noted above in the Methods section, we also observed several trials of quadrupedal locomotion in which monkeys actively used the tail to grasp the substrate. This behavior was particularly common in the atelines (i.e., *Alouatta, Ateles*, and *Lagothrix*) and preliminary analyses suggest active tail grasping was more common on narrower and more angled supports. Given that active tail prehension would offer an alternative means of maintaining arboreal stability, we ultimately excluded such trials from our kinematic analyses of tail dynamics as being outside the primary focus of this study. Nevertheless, we hope to explore this phenomenon in future studies of this dataset.

Limitations

The sample size for our captive squirrel monkey study was necessarily limited by the logistical difficulties of obtaining and housing nonhuman

primates. Although we made efforts to generate a robust dataset by sampling many strides per individual, the low number of individuals has the potential to bias results, particularly in cases where the two individuals show differing patterns of variation. However, ICCs in our dataset were generally low—across the eight linear models used to analyze squirrel monkey tail mechanics, the mean ICC was 0.163, indicating that on average only 16% of dependent measure variation was due to performance differences between the two monkeys. Moreover, we explicitly used hierarchical mixed-effects modeling as a means of controlling for interindividual variance when testing predictions. Such models are functionally equivalent to repeated measures designs, testing how our variables of interest impacted tail kinematics within each monkey. Future studies should extend this work by examining tail kinematics in arboreal quadrupeds that are more readily sampled (e.g., *Anolis* lizard).

Conclusions

The data presented support the hypothesis that a biological role for the long tails of arboreal animals is to serve as a free inertial appendage that can promote stability when moving quadrupedally over narrow and mobile substrates. Tail angular momentum could be used to cancel out the angular momentum generated by other parts of the body, thereby reducing whole-body angular momentum during steady-state progression, and could be used to mitigate the effects of destabilizing torques about the support should the animals encounter large, unexpected perturbations. Of course, promoting stability during arboreal quadrupedalism is not the only potential biological role of a long and mobile tail, nor even the only locomotor-related role. Several studies have demonstrated leaping and falling animals use tail angular momentum as an effective means of reorienting the body in space, thus facilitating a safe landing (*Dunbar* 1988; *Demes* et al. 1996; *Akatani* et al. 2000; *Walker* 2005; *Jusufi* et al. 2008; *Gillis* et al. 2009; *Libby* et al. 2012). Nonlocomotory functions of the tail can include social displays and thermoregulation (*Hickman* 1979; *Mincer* and Russo 2020). Nevertheless, our findings suggest that long mobile tails should be considered among the suite of fundamental arboreal adaptations promoting safe and efficient above-branch locomotion.

Future research should directly consider how changes in tail angular momentum interact with segmental angular momentum changes from more cranial body segments, directly quantifying the degree to which tail momentum has the potential to contribute to whole-body momentum control (*Herr* and Popovic 2008; *Chiovetto* et al. 2018). Additionally, it would be instructive to test for other morphological differences between arboreal and terrestrial taxa that might promote "tail performance" during locomotion on precarious arboreal supports. For example, arboreal species might have a greater number of caudal vertebrae for a given tail length, promoting increased mobility for a given muscle contraction (*Lemelin* 1995). Arboreal taxa may have more powerful caudal musculature (i.e., greater physiological cross-sectional areas and or longer muscle fibers) relative to closely related terrestrial taxa, facilitating high-velocity tail movements. Finally, future research should extend beyond primates, establishing the degree to which the functional associations documented here may be representative of tail usage in other arboreal tetrapods.

Data availability statement

All data presented in our analyses are available as comma-delimited (.csv) files in the online Supplementary Materials.

Acknowledgments

We thank Timothy O'Neill, Kyle Resnick, and Bethany Stricklen for data collection and analysis of the laboratory *S. boliviensis* dataset, and the NEOMED Comparative Biomechanics Laboratory for feedback on prior iterations of this research; the Universidad San Francisco de Quito, Tomi Sugahara, Diego Mosquera, Gabriela Vinueza, Anthony Di Fiore, Max Snodderly, Krista Milich, Laura Abondano, Natalia Camargo, Sam Rettke, Savannah Perez, Jacopo Cantoni, Laura Gómes, Cristian Alvarado, Renee Peters, and TBS staff who provided invaluable scientific and logistical support; Renee Molina for facilitating research at La Suerte and to Michelle Bezanson for logistical support; and the two external reviewers for their helpful comments and suggestions.

Funding

Research supported by National Science Foundation grants BCS-1126790, BCS-1640552, BCS-1640453, and BCS-1921135 and by NEOMED Department of Anatomy and Neurobiology.

Supplementary data

Supplementary Data available at *ICB* online.

References

Akatani J, Wada N, Tokuriki M. 2000. Electromyographic and kinematic studies of tail movements during falling in cats. Arch Ital Biol 138:271–5.

Almécija S, Alba DM, Moyà-Solà S, Köhler M, Kohler. 2007. Orang-like manual adaptations in the fossil hominoid *Hispanopithecus laietanus*: first steps towards great ape suspensory behaviours. Proc Royal Soc Lond B Biol Sci 274:2375–84.

Arnold C, Matthews LJ, Nunn CL. 2010. The 10kTrees website: A new online resource for primate phylogeny. Evol Anthropol 19:114–8.

Ballinger RE. 1973. Experimental evidence of the tail as a balancing organ in the lizard *Anolis carolinensis*. Herpetologica 29:65–6.

Basu C, Wilson AM, Hutchinson JR. 2019. The locomotor kinematics and ground reaction forces of walking giraffes. J Exp Biol 222:jeb159277

Begun DR, Teaford MF, Walker A. 1994. Comparative and functional anatomy of *Proconsul* phalanges from the Kaswanga Primate Site, Rusinga Island, Kenya. J Human Evol 26:89–165.

Boinski S. 1989. The positional behavior and substrate use of squirrel monkeys: ecological implications. J Human Evol 18:659–77.

Briggs R, Lee J, Haberland M, Kim S. 2012. Tails in biomimetic design: analysis, simulation, and experiment. In: 2012 IEEE/RSJ International Conference on Intelligent Robots and Systems. IEEE. p. 1473–80.

Buck CW, Tolman N, Tolman W. 1925. The tail as a balancing organ in mice. J Mammal 6:267–71.

Cartmill M, Lemelin P, Schmitt D. 2007. Primate gaits and primate origins. In: Ravosa MJ, Dagosto M, editors. Primate origins: adaptations and evolution. New York (NY): Springer. p. 403–35.

Cartmill M, Milton K. 1977. The lorisiform wrist joint and the evolution of ''brachiating''adaptations in the Hominoidea. Am J Phys Anthropol 47:249–72.

Chadwell BA, Young JW. 2015. Angular momentum and arboreal stability in common marmosets (*Callithrix jacchus*). Am J Physical Anthropol 156:565–76.

Chiovetto E, Huber ME, Sternad D, Giese MA. 2018. Low-dimensional organization of angular momentum during walking on a narrow beam. Sci Rep 8:1–14.

Collins SH, Adamczyk PG, Kuo AD. 2009. Dynamic arm swinging in human walking. Proc Royal Soc B Biol Sci 276:3679–88.

Crawley MJ. 2007. The R Book. West Sussex, UK: John Wiley and Sons, Ltd.

Delciellos AC, Vieira MV. 2007. Stride lengths and frequencies of arboreal walking in seven species of didelphid marsupials. Acta Theriol 52:101–11.

Demes B, Jungers WL, Fleagle JG, Wunderlich RE, Richmond BG, Lemelin P. 1996. Body size and leaping kinematics in Malagasy vertical clingers and leapers. J Hum Evol 31:367–88.

Diniz FJ, Villalobos F, Bini LM. 2015. The best of both worlds: phylogenetic eigenvector regression and mapping. Genet Mol Biol 38:396–400.

Dunbar DC. 1988. Aerial maneuvers of leaping lemurs: he physics of whole-body rotations while airborne. Am J Primatol 16:291–303.

Dunham NT, McNamara A, Shapiro LJ, Hieronymus TL, Phelps T, Young JW. 2019a. Effects of substrate and phylogeny on quadrupedal gait in free-ranging platyrrhines. Am J Phys Anthropol 170:565–78.

Dunham NT, McNamara A, Shapiro LJ, Hieronymus TL, Young JW. 2018. A user's guide for the quantitative analysis of substrate characteristics and locomotor kinematics in free-ranging primates. Am J Phys Anthropol 167:569–84.

Dunham NT, McNamara A, Shapiro LJ, Phelps T, Wolfe AN, Young JW. 2019b. Locomotor kinematics of tree squirrels (*Sciurus carolinensis*) in free-ranging and laboratory environments: implications for primate locomotion and evolution. J Exp Zool A Ecol Genet Physiol 331:103–19.

Dunham NT, McNamara A, Shapiro LJ, Phelps T, Young JW. 2020. Asymmetrical gait kinematics of free-ranging callitrichines in response to changes in substrate diameter and orientation. J Exp Biol 223:jeb217562.

Elftmann H. 1939. The function of the arms in walking. Hum Biol 11:529–35.

Garber PA, Molina A, Molina RL. 2010. Putting the community back in community ecology and education: the role of field schools and private reserves in the ethical training of primatologists. Am J Primatol 72:785–93.

Gillis GB, Bonvini LA, Irschick DJ. 2009. Losing stability: tail loss and jumping in the arboreal lizard *Anolis carolinensis*. J Exp Biol 212:604–9.

Grand TI. 1977. Body weight: its relation to tissue composition, segment distribution, and motor function. I. Interspecific comparisons. Am J Phys Anthropol 47:211–39.

Hayssen V. 2008. Patterns of body and tail length and body mass in Sciuridae. J Mamm 89:852–73.

Herr H, Popovic M. 2008. Angular momentum in human walking. J Exp Biol 211:467–81.

Hickman GC. 1979. The mammalian tail: a review of functions. Mamm Rev 9:143–57.

Horner E. 1954. Arboreal adaptations of *Peromyscus*, with special reference to use of the tail. In: Contributions from the laboratory of vertebrate biology, Series 61. Ann Arbor, MI: University of Michigan. p. 1–84.

Hsieh S-TT. 2016. Tail loss and narrow surfaces decrease locomotor stability in the arboreal green anole lizard (*Anolis carolinensis*). J Exp Biol 219:364–73.

Igarashi M, Levy JK. 1981. Locomotor balance performance of short-tailed squirrel monkeys. J Med Primatol 10:136–40.

Irschick DJ, Vitt LJ, Zani PA, Losos JB. 1997. A comparison of evolutionary radiations in mainland and Caribbean *Anolis* lizards. Ecology 78:2191–203.

Jenkins FA. 1974. Tree shrew locomotion and the origins of primate arborealism. In: Jenkins FA, editor. Primate locomotion. New York and London: Academic Press. p. 85–115.

Jusufi A, Goldman DI, Revzen S, Full RJ. 2008. Active tails enhance arboreal acrobatics in geckos. Proc Natl Acad Sci 105:4215–9.

Jusufi A, Zeng Y, Full RJ, Dudley R. 2011. Aerial righting reflexes in flightless animals. Integr Comp Biol 51:937–43.

Kelley J. 1997. Paleobiological and phylogenetic signal of life history in Miocene hominoids. In: Begun DR, Ward CV, Rose MD, editors. Function, phylogeny, and fossils: miocene hominoid evolution and adaptations. New York, NY: Plenum Press. p. 173–208.

Larson SG. 1998. Unique aspects of quadrupedal locomotion in nonhuman primates. In: Strasser E, Fleagle J, Rosenberger A, McHenry H, editors. Primate locomotion: ecent advances. New York, NY: Plenum Press. p. 157–73.

Larson SG, Stern JT. 2006. Maintenance of above-branch balance during primate arboreal quadrupedalism: coordinated use of forearm rotators and tail motion. Am J Phys Anthropol 129:71–81.

Lemelin P. 1995. Comparative and functional myology of the prehensile tail in New World monkeys. J Morphol 224:351–68.

Lemelin P, Schmitt D. 2007. Origins of grasping and locomotor adaptations in primates: comparative and experimental approaches using an opossum model. In: Ravosa MJ, Dagosto M, editors. Primate origins: adaptations and evolution. New York, NY: Springer. p. 329–80.

Libby T, Moore TY, Chang-Siu E, Li D, Cohen DJ, Jusufi A, Full RJ. 2012. Tail-assisted pitch control in lizards, robots and dinosaurs. Nature 481:181–4.

Marsh LK. 2004. Primate species at the Tiputini biodiversity station, Ecuador. Neotrop Primates 12:75–8.

Martin RD. 1968. Reproduction and ontogeny in tree-shrews (*Tupaia belangeri*), with reference to the general behaviour and taxonomic relationships. Z Tierpsychol 25:409–95.

McNamara A, Dunham NT, Shapiro LJ, Young JW. 2019. The effects of natural substrate discontinuities on the quadrupedal gait kinematics of free-ranging *Saimiri sciureus*. Am J Primatol 81:e23055.

Mincer ST, Russo GA. 2020. Substrate use drives the macroevolution of mammalian tail length diversity. Proc Royal Soc B 287:20192885.

Mittermeier RA, Rylands AB, Wilson DE. 2013. Handbook of mammals of the world. Barcelona, Spain: Lynx Editions.

Nakagawa S, Johnson PC, Schielzeth H. 2017. The coefficient of determination R 2 and intra-class correlation coefficient from generalized linear mixed-effects models revisited and expanded. J Royal Soc Interf 14:20170213.

Nyakatura JA. 2019. Early primate evolution: insights into the functional significance of grasping from motion analyses of extant mammals. Biol J Linn Soc 127:611–31.

Patel A, Braae M. 2013. Rapid turning at high-speed: inspirations from the cheetah's tail. In: 2013 IEEE/RSJ International Conference on Intelligent Robots and Systems. IEEE. p. 5506–11.

Pontzer H, Holloway JH, Holloway JH, Raichlen DA, Lieberman DE. 2009. Control and function of arm swing in human walking and running. J Exp Biol 212:523–34.

Raichlen DA. 2004. Convergence of forelimb and hindlimb Natural Pendular Period in baboons (*Papio cynocephalus*) arid its implication for the evolution of primate quadrupedalism. J Hum Evol 46:719–38.

Rose MD. 1974. Postural adaptations in New and Old World monkeys. In: Jenkins FA, editor. Primate locomotion. New York, NY: Academic Press. p. 201–22.

Russell AP, Stark AY, Higham TE. 2019. The integrative biology of gecko adhesion: historical review, current understanding, and grand challenges. Integr Comp Biol 59:101–16.

Russo GA, Shapiro LJ. 2011. Morphological correlates of tail length in the catarrhine sacrum. J Human Evol 61:223–10.

Schmitt D, Cartmill M, Griffin T, Hanna, MJB, Lemelin, P. 2006. Adaptive value of ambling gaits in primates and other mammals. J Exp Biol 209:2042–9.

Sehner S, Fichtel C, Kappeler PM. 2018. Primate tails: Ancestral state reconstruction and determinants of interspecific variation in primate tail length. Am J Phys Anthropol 167:750–9.

Shapiro LJ, Chadwell BA, Young JW. 2016. Tail kinematics during asymmetrical gaits in mouse lemurs (*Microcebus murinus*). Am J Phys Anthropol 159: 38.

Shapiro LJ, Young JW, VandeBerg JL. 2014. Body size and the small branch niche: using marsupial ontogeny to model primate locomotor evolution. J Hum Evol 68:14–31.

Sheehy IIC, Albert JS, Lillywhite HB. 2016. The evolution of tail length in snakes associated with different gravitational environments. Functl Ecol 30:244–54.

Siegel MI, van Meter R. 1973. Skeletal correlates of ecological adaptation in two species of *Peromyscus*. J Mamm 54:275–8.

Smith RJ, Jungers WL. 1997. Body mass in comparative primatology. J Hum Evol 32:523–59.

Standen EM, Lauder GV. 2005. Dorsal and anal fin function in bluegill sunfish *Lepomis macrochirus*: three-dimensional kinematics during propulsion and maneuvering. J Exp Biol 208:2753–63.

Wada N, Hori H, Tokuriki M. 1993. Electromyographic and kinematic studies of tail movements in dogs during treadmill locomotion. J Morphol 217:105–13.

Walker C, Vierck CJ, Ritz LA. 1998. Balance in the cat: role of the tail and effects of sacrocaudal transection. Behav Brain Res 91:41–7.

Walker SE. 2005. Leaping behavior of *Pithecia pithecia* and *Chiropotes satanas* in eastern Venezuela. Am J Primatol 66:369–87.

Weisbecker V, Speck C, Baker AM. 2020. A tail of evolution: evaluating body length, weight and locomotion as potential drivers of tail length scaling in Australian marsupial mammals. Zool J Linn Soc 188:242–54.

Wilson DR. 1972. Tail reduction in *Macaca*. In: Tuttle RH, editor. The functional and evolutionary biology of primates. Chicago, IL: Aldine-Atherton. p. 241–61.

Young JW. 2012. Ontogeny of limb force distribution in squirrel monkeys (*Saimiri boliviensis*): insights into the mechanical bases of primate hind limb dominance. J Hum Evol 62:473–85.

Young JW, Chadwell BA. 2020. Not all fine-branch locomotion is equal: Grasping morphology determines locomotor performance on narrow supports. J Hum Evol 142:102767.

Young JW, Russo GA, Fellmann CD, Thatikunta MA, Chadwell BA. 2015. Tail function during arboreal quadrupedalism in squirrel monkeys (*Saimiri boliviensis*) and tamarins (*Saguinus oedipus*). J Exp Zool A Ecol Genet Physiol 323:556–66.

Young JW, Stricklen BM, Chadwell BA. 2016. Effects of support diameter and compliance on common marmoset (*Callithrix jacchus*) gait kinematics. J Exp Biol 219:2659–72.

Zimbler-Delorenzo HS, Stone AI. 2011. Integration of field and captive studies for understanding the behavioral ecology of the squirrel monkey (Saimiri sp.). Am J Primatol 73:607–22.